Geophysical Research Letters

RESEARCH LETTER
10.1029/2024GL113338

Australian Heritage for the North Lhasa Terrane

Chang-Sheng Yu[1], Ming Wang[1,2], Jian-Bo Zhou[1], Richard M. Palin[3], Jin Liu[1], Bin Wan[4], Di Shen[1], Quewang Danzeng[1], and Sheng-Shuo Zhang[1]

[1]College of Earth Sciences, Jilin University, Changchun, China, [2]Key Laboratory of Mineral Resources Evaluation in Northeast Asia, Ministry of Land and Resources, Changchun, China, [3]Department of Earth Sciences, University of Oxford, Oxford, UK, [4]State Key Laboratory of Palaeobiology and Stratigraphy, Nanjing Institute of Geology and Palaeontology, Chinese Academy of Sciences, Nanjing, China

Key Points:

- Newly identified 2.62 Ga granites in the North Lhasa terrane show affinity with the Pilbara Craton, Western Australia
- The 1.30–1.10 Ga Guomangtso Suite identified in North Lhasa documents the Proterozoic assembly of North and West Australian Cratons
- The North Lhasa terrane was connected with Western Australia before separating during the Neoproterozoic

Supporting Information:

Supporting Information may be found in the online version of this article.

Correspondence to:

M. Wang and J.-B. Zhou,
wm609@163.com;
zhoujianbo@jlu.edu.cn

Citation:

Yu, C.-S., Wang, M., Zhou, J.-B., Palin, R. M., Liu, J., Wan, B., et al. (2025). Australian heritage for the North Lhasa terrane. *Geophysical Research Letters*, *52*, e2024GL113338. https://doi.org/10.1029/2024GL113338

Received 30 OCT 2024
Accepted 2 FEB 2025

Author Contributions:

Conceptualization: Chang-Sheng Yu
Data curation: Di Shen
Formal analysis: Chang-Sheng Yu
Funding acquisition: Ming Wang
Investigation: Bin Wan
Methodology: Di Shen
Project administration: Di Shen
Resources: Quewang Danzeng, Sheng-Shuo Zhang
Supervision: Ming Wang, Jian-Bo Zhou, Richard M. Palin, Jin Liu, Bin Wan
Writing – original draft: Chang-Sheng Yu
Writing – review & editing: Ming Wang, Richard M. Palin, Jin Liu

Abstract The Precambrian history of the Lhasa terrane, southern Tibet is intensely debated, which hinders global plate tectonic reconstructions throughout the Proterozoic. Previous research on Precambrian basement has suggested that the Lhasa terrane originated from India or Africa, although the paucity of exposed pre-Neoproterozoic rocks in the North Lhasa terrane (NL) has led to significant uncertainty. We document newly identified Neoarchean granites and Mesoproterozoic Guomangtso Suite from the NL. These pre-Neoproterozoic rocks reveal a 2.62 Ga anorogenic rifting event and a 1.30–1.10 Ga transition from subduction to back-arc extension, related to the 2.7–2.6 Ga rifting of the Pilbara Craton and the Proterozoic assembly between the North and West Australian Cratons, respectively. However, these tectono-magmatic events have no equivalents in the South Lhasa terrane (SL). These observations suggest that the NL originated from Western Australia, and the NL and SL may have distinct origins.

Plain Language Summary Constraining the origin and evolution of continental fragments plays a crucial role in validating the patterns in the growth of successive supercontinents. However, tracking the evolving paleogeographic position of these fragments, especially for those of Precambrian age without paleolongitude constraints, has proven difficult. We redefine the pre-Neoproterozoic evolution of the Lhasa terrane, southern Tibet based on newly discovered Neoarchean and Mesoproterozoic rocks, which contain missing information about the pre-Neoproterozoic evolution of the North Lhasa terrane (NL). We reveal the Neoarchean–Mesoproterozoic evolution of the NL and its affinity with Western Australia, which is clearly distinct from the Indian affinities of the South Lhasa terrane (SL) from the Paleoproterozoic to Mesoproterozoic. These findings suggest that the Lhasa terrane did not originate as a unified entity from India during the pre-Neoproterozoic, as previously thought, but rather that the NL originated from Western Australia, with the NL and SL having distinct origins. Our study therefore shows for the first time key evidence identifying the origin of the NL before the Neoproterozoic.

1. Introduction

The Qinghai–Tibet Plateau is the youngest and highest plateau on Earth, and intense multi-disciplinary study over several decades has led to significant advances in understanding its formation and evolution. However, the geological history of the Lhasa terrane—the southernmost of three large east—west-trending tectonic belts in the plateau (Figure 1a)—remains obscure, hindering plate tectonic reconstructions throughout the Phanerozoic and Proterozoic. Traditional views posit that the Lhasa terrane rifted away from Indian Gondwana before its collision with the Qiangtang terrane during the Mesozoic (Figure 1b; Gehrels et al., 2011) or as part of the Late Cambrian to Early Paleozoic evolution of Australian Gondwana (Figure 1c; Zhu et al., 2011). Evidence for both viewpoints stems from detrital zircon data for Paleozoic sedimentary rocks, yet they yield different conclusions (Hu, Zhai, Zhao, et al., 2022). Recent studies have shown that the Lhasa terrane exhibits an African (Northern East African Orogen) affinity based on the occurrence of 650 Ma HP granulites and detrital zircon REE profiles (Figure 1d; Hu et al., 2023; Zhang et al., 2012). However, Zhang et al. (2022) suggested that the Lhasa terrane is the "lost" part of NW India, with its 760–730 Ma ophiolitic-arc magmatic rocks representing part of the Neoproterozoic suprasubduction-zone arc–backarc systems along the western periphery of the Rodinia supercontinent. Additionally, our previous work has reported early Neoproterozoic intercontinental rift magmatic-sedimentary records in the NL, possibly related to equivalent units in Western Australia (Yu et al., 2024). In brief, conclusions derived from the geological records preserved in Neoproterozoic basement rocks of the Lhasa terrane are contradictory, making it difficult to constrain its tectonic history and origin.

Although paleogeographic reconstructions using detrital zircon have proven effective (Veevers et al., 2005), their application to the Lhasa terrane has caused ambiguity. This is mainly due to different results obtained from Paleozoic sedimentary rock detrital zircon data (e.g., Gehrels et al., 2011; Zhu et al., 2011). Magmatic records are thus crucial for supporting paleogeographic reconstructions, especially for Precambrian terranes like the Lhasa terrane, which lack paleomagnetic data for precise geolocation (e.g., Cawood et al., 2018; Li et al., 2008). The Nyainqentanglha Group, the Precambrian basement of the NL, primarily contains Neoproterozoic lithologies that have recently been shown to exhibit affinities with units in India, Australia, and Africa (e.g., Hu et al., 2023; Yu et al., 2024; Zhou et al., 2019). The presence of multiple affinities makes it difficult to determine the origin of the Lhasa terrane solely through Neoproterozoic geological records. The scarcity of pre-Neoproterozoic basement of the NL further hampers our understanding of the Lhasa terrane's origin and its place in global plate tectonic reconstructions through time.

Here, we document Mesoproterozoic felsic and mafic magmatic rocks (the Guomangtso Suite) and Neoarchean granites that have been newly identified from the NL. We present whole-rock geochemistry, zircon U–Pb geochronology, and zircon Lu–Hf and whole-rock Sr–Nd–Pb isotopic analyses. These data reveal the pre-Neoproterozoic evolutionary history of the NL and propose a progressive model for the origin and evolution of the entire Lhasa terrane between 3.0 and 1.0 Ga. Our results have implications for paleogeographic reconstructions during the Proterozoic, and for understanding the tectonic evolution of southern Tibet and northwestern Rodinia.

2. Geological Background, and Field Occurrence of Neoarchean and Mesoproterozoic Magmatic Rocks

The Lhasa terrane, situated between the South Qiangtang and Himalayan terranes, is divided into NL and SL by the Sumdo (Paleo-Tethys) suture zone (Figure 1a; Chen et al., 2022). The Precambrian basements of the NL and SL are termed the Nyainqentanglha Group and Nyingchi Complex, respectively (Figure 1a; Chen et al., 2022; Hu et al., 2018b). The Nyainqentanglha Group (NL) is dominated by Neoproterozoic rocks, without evidence for Mesoproterozoic magmatic activity, while the Nyingchi Complex (SL) contains Paleoproterozoic to Mesoproterozoic magmatic and metamorphic records, but lacks any evidence for Neoproterozoic rock units or events (Chen et al., 2022; Yu et al., 2023, 2024). The former mainly records: (a) ∼900 Ma rift-related magmatic-sedimentary rocks (Hu et al., 2018c); (b) 839–806 Ma back-arc basin units (Hu et al., 2018a; Zhou et al., 2019); (c) 760–730 Ma arc-related magmatic rocks and oceanic crust fragments (Hu et al., 2018b; Zhang et al., 2022); (d) 658–646 Ma continent-continent collision-related magmatism and metamorphism (Hu, Zhai, Cawood, et al., 2022; Hu, Zhai, Zhao, Wang, et al., 2019; Zhang et al., 2012); and (e) 572–541 Ma arc magmatic rocks (Hu et al., 2018d, 2021). In contrast, the latter mainly records: (a) 1866–1782 Ma and 1556–1506 Ma subduction-collision events (Chen et al., 2019; Dong et al., 2020, 2022; Lin et al., 2013); (b) 1343–1276 Ma continental rifting (Xu et al., 2013); (c) 1264–1250 Ma arc magmatism related to the Grenvillian orogeny, along with ∼1200 Ma metamorphism (Chen et al., 2019; Dong et al., 2022). Therefore, direct comparison of the Precambrian basements of the NL and SL cannot be made.

Here, we report newly identified Neoarchean granites within the Lagar Formation (Late Carboniferous–Early Permian, Ma et al., 2015; Wang et al., 2020), located in the Asa area of the NL (Figure 1a). The glacial sediments of the Lagar Formation were deposited near a grounding line or ice front in littoral-neritic to neritic environments (Ma et al., 2020; Zhang et al., 2013). These granites occur as dense fields of boulders with sizes up to 1.5 × 1.0 m, and are associated with ripple marks and biolithic limestone intercalations in their host rocks (Figure S1 in Supporting Information S1). The granites are pink-brown and massive, and contain plagioclase (35%), microcline (25%), K-feldspar (20%), quartz (15%), with minor riebeckite and sericite.

Mesoproterozoic felsic (granitoid) and mafic (amphibolite) rocks, termed the Guomangtso Suite, have also been newly identified in the NL. These rocks occur as blocks or tectonic slices ranging in thickness from a few hundred meters to tens of kilometers (Figure S2 in Supporting Information S1), although their contacts with the surrounding Paleozoic strata are obscured due to extensive coverage by Quaternary sediments. The granitoids are primarily composed of quartz (30%–60%), plagioclase (10%–20%), microcline (5%–15%), sericite (5%–10%), with minor biotite, whereas the amphibolites contain amphibole (40%–60%), plagioclase (10%–25%), quartz (5%–10%), and sericite (5%).

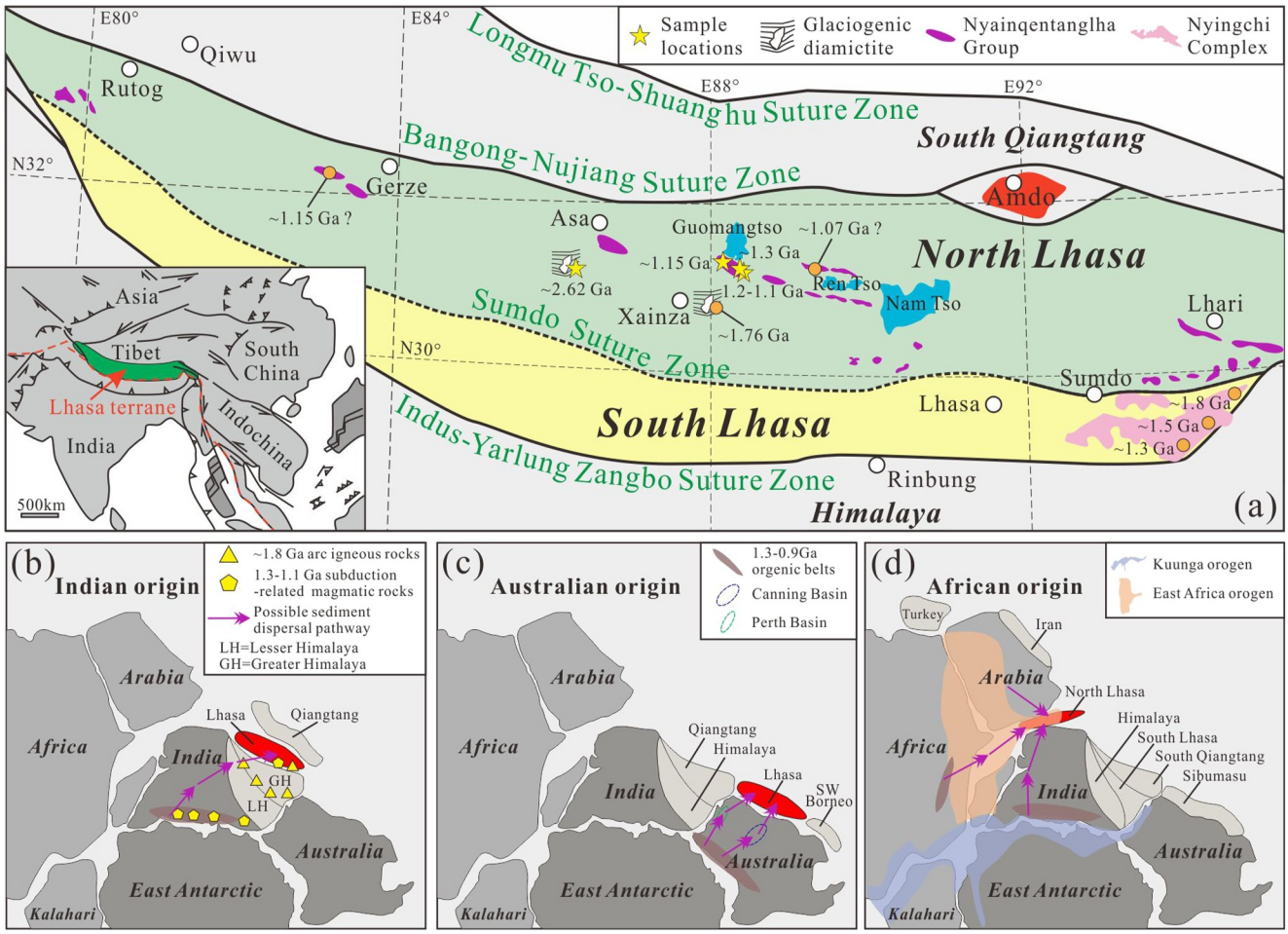

Figure 1. (a) Tectonic framework of southern Tibet (after Ma et al., 2020; Hu et al., 2023; Yu et al., 2024). (b–d) Three major models showing the paleogeographic proximity of the North Lhasa terrane to India (Chen et al., 2019; Gehrels et al., 2011; Zhou et al., 2019), Australia (Wang et al., 2021; Zhu et al., 2011), and Africa (Hu, Zhai, Zhao, Tang, et al., 2019; Hu et al., 2018b; Zhang et al., 2012).

3. Geochronological and Geochemical Results

To establish the geochronological framework of the NL, we conducted U–Pb analyses of 283 zircons from 15 samples (five for each type, detailed sample locations and zircon U–Pb age results are shown in Table S1 in Supporting Information S1). Detailed descriptions of the acquisition of zircon U–Pb age data and Hf isotopes, whole-rock geochemistry and Sr–Nd–Pb data, are provided in the Supporting Information S1. The results reveal at least seven discrete magmatic episodes at 3.0, 2.6, 1.9, 1.8–1.7, 1.5, 1.3, and 1.2–1.1 Ga (Figure 2a). A series of Mesoarchean–Mesoproterozoic magmatic events are recorded by numerous 3.0–1.3 Ga xenocrystic zircons found within the younger Guomangtso Suite (1.3–1.1 Ga). These xenocrysts exhibit concentric oscillatory internal zonation, suggesting crystallization from a felsic melt (Figures 2b and 2c). The 3.0–2.8 Ga magma pulses are consistent with those recorded in the Archean Pilbara Craton, Western Australia (Figure 2a). Evidence for subsequent Neoarchean–early Paleoproterozoic magmatic events is provided by 2.62 Ga granites and 2.7–2.3 Ga xenocrystic zircons within the Guomangtso Suite (Figure 2a), with these 2.62 Ga granites being the oldest rocks documented in Tibet. Late Paleoproterozoic magmatic events (2.0–1.6 Ga) are evidenced by 1.76 Ga granites from the Xinaza area (Ma et al., 2020), and 2.0–1.6 Ga xenocrystic zircons within the Guomangtso Suite (Figure 2a). Finally, three episodes of Mesoproterozoic magmatism are documented by 1.5–1.3 Ga xenocrystic zircons and the Guomangtso Suite, similar to those in the Rudall Province and Pilbara Craton, Western Australia (Figure 2a).

We also analyzed 25 samples for major and trace elements (nine Neoarchean granite samples, and seven granitoid and nine amphibolite samples of Mesoproterozoic age). Whole-rock major- and trace-element data are

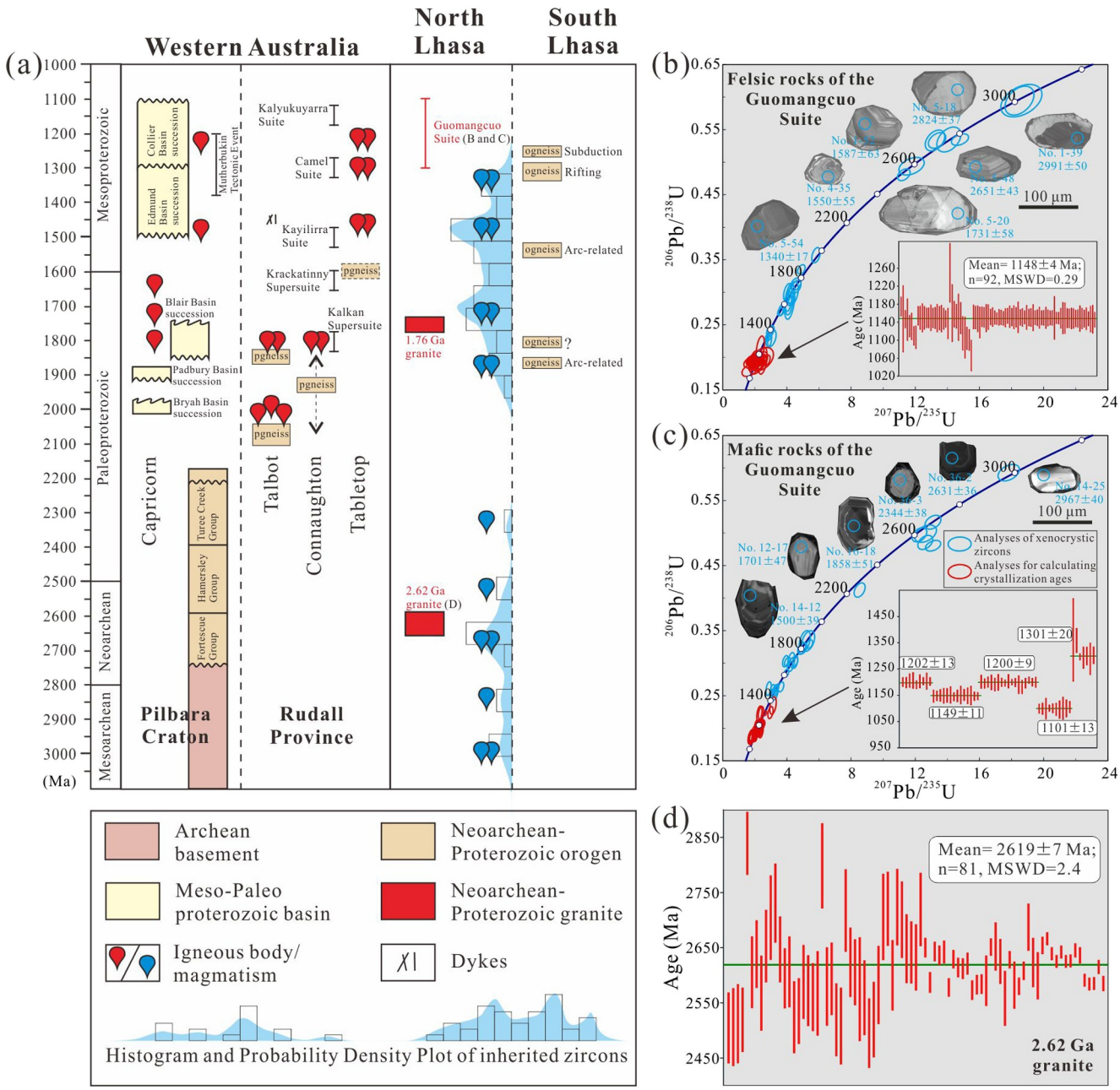

Figure 2. (a) Time-space diagram illustrating the age range of lithotectonic units and the timing of tectonothermal events in Western Australia and the Lhasa terrane (adapted from Cawood & Korsch, 2008; Chen et al., 2019; Cutten et al., 2011; Dong et al., 2022; Gardiner et al., 2018; Ma et al., 2020; Martin & Thorne, 2004; Payne et al., 2021). (b–d) Zircon U-Pb dating results for Neoarchean granites and Mesoproterozoic felsic and mafic rocks in the North Lhasa terrane.

given in Table S2 in Supporting Information S1. The 2.62 and 1.15 Ga granitoids exhibit similar geochemical features, such as enrichment in light rare earth elements (e.g., La, Ce, and Pr) and Zr, but depletion in heavy rare earth elements (e.g., Lu, and Yb), Nb, and Ta (Figure 2a). The 2.62 Ga granites have high SiO_2 (69.1–74.8 wt.%), low MgO (0.58–1.23 wt.%), $Fe_2O_3^T$ (3.57–5.32 wt.%), Cr (2.94–6.49 ppm), and Ni (3.34–19.40 ppm) contents, and are ferroan, alkali-rich and Ga, Zr, REE-rich, akin to anorogenic/A-type rocks (Whalen et al., 1987). On a Rb–(Y + Nb) diagram (Figure S4 in Supporting Information S1), the 2.62 Ga granites plot within the field of within-plate granite. In contrast, the 1.15 Ga granitoids show a wide range of SiO_2 (65.9–85.5 wt.%), MgO (0.75–2.65 wt.%), $Fe_2O_3^T$ (1.05–6.32 wt.%), Cr (30.4–85.3 ppm), and Ni (13.8–38.7 ppm) contents, and are peraluminous, consistent with crustally derived granitoids (Figure S4 in Supporting Information S1). The

10.1029/2024GL113338

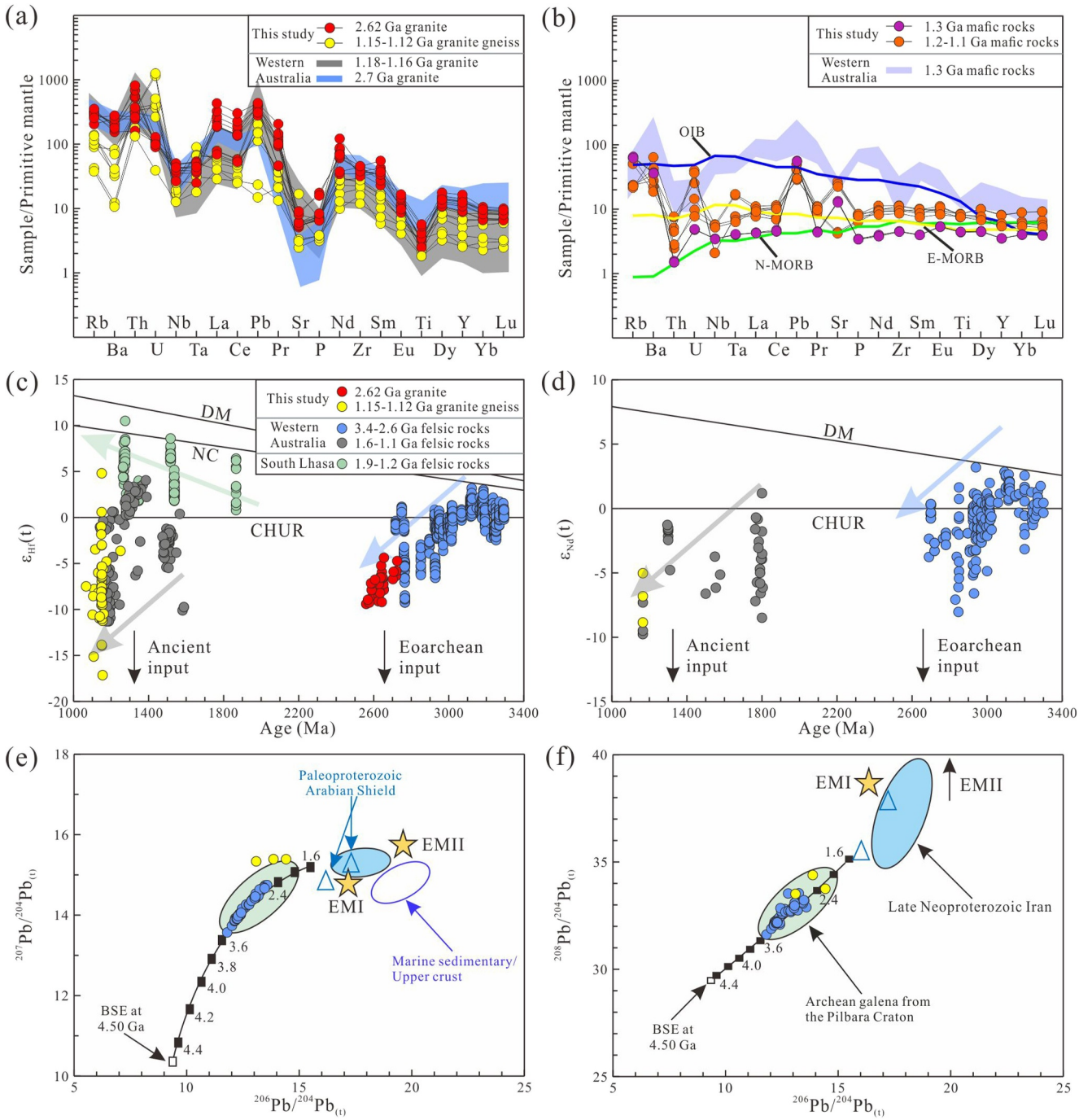

Figure 3. Geochemical and isotopic characteristics of the studied samples. (a, b) Primitive mantle-normalized multi-element patterns. (c–f) Zircon Hf and whole-rock Nd-Pb isotopic composition. The new crust (NC) reference curve is calculated using parameters from Dhuime et al. (2011). Data compiled from various published studies, including Stoeser and Frost (2006), Gardiner et al. (2017), Honarmand et al. (2018), Hawkesworth and Kemp (2021), Payne et al. (2021), Dong et al. (2022), Hartnady et al. (2022), and Kemp et al. (2023).

1.3–1.1 Ga amphibolites are classified as tholeiitic basalts. Their enrichment in large ion lithophile elements (e.g., Rb, Ba, Sr, and Pb) (Figure 2a) and low Nb/La ratios (0.28–0.84) potentially indicate crustal contamination (Nb/La <1; Kieffer et al., 2004). All amphibolites samples show affinities to MORB (Figure 3b). However, 1.2–1.1 Ga samples notably show geochemical characteristics of continental flood basalts and within-plate basalts,

whereas 1.3 Ga samples display geochemical traits indicative of arc-related magmatic rocks (Figure S4 in Supporting Information S1).

We performed 75 new zircon Hf isotope analyses for the 2.62 and 1.15 Ga granitoids. The zircon Hf isotope results are presented in Table S3 in Supporting Information S1. The negative zircon $\varepsilon_{Hf}(t)$ values (−4.35 to −9.37) indicate the 2.62 Ga granites are dominated by non-radiogenic Hf, consistent with a crustal magma source. Ancient two-stage model ages (3.7–3.4 Ga) show that they are the products of recycling of pre-existing crust. The 1.15 Ga granitoids exhibit a wide range of $\varepsilon_{Hf}(t)$ values (−17.5 to 4.8), indicative of progressive isotopic dilution of Archean crust by Paleoproterozoic and Mesoproterozoic magmatism (e.g., the Kalyukuyarra Suite, Payne et al., 2021). Additionally, three new whole-rock Sr–Nd–Pb isotope data for the 1.15 Ga granitoids ($^{87}Sr/^{86}Sr$ = 0.7284–0.7483; $\varepsilon_{Nd}(t)$ = −4.6 to −2.5; $^{206}Pb/^{204}Pb$ = 19.77–20.52; $^{207}Pb/^{204}Pb$ = 15.85–15.89; $^{208}Pb/^{204}Pb$ = 40.99–42.61, Table S4 in Supporting Information S1) are similar to those of granitic plutons of the Shaw Batholith in the Archean Pilbara Craton (e.g., Bickle et al., 1989).

4. Discussion

4.1. Magmatic Affinity Between the North Lhasa Terrane and Western Australia

Zircon Hf isotope characteristics indicate that the pre-Neoproterozoic crystalline basement of the NL is primarily derived from ancient crustal recycling, akin to Western Australia (Figure 3c). In contrast, the SL is predominantly composed of mantle-derived magmas or juvenile continental crust (Figure 3c). The Guomangtso Suite identified in the NL, which includes 1.15–1.12 Ga peraluminous crustally derived granites and MORB-like amphibolites (1.3 Ga arc-related basalts and 1.2–1.1 Ga continental flood basalts), suggests a transition from subduction to back-arc extension. This setting parallels oceanic crust subduction beneath the northern and eastern margins of Western Australia at 1380–1250 Ma and subsequent extension (1185–1165 Ma) that led to formation of the Kalyukuyarra Suites in the Rudall Province of Western Australia (Figure 2a; Gardiner et al., 2018; Payne et al., 2021); however, it contrasts with 1343–1276 Ma aluminous A-type granites formed in a continental rift setting and 1250–1117 Ma subduction-related magmatism and metamorphism in the SL (Chen et al., 2019; Dong et al., 2022; Xu et al., 2013). Although Late Paleoproterozoic subduction-related magmatism has been reported in both the SL and NL (e.g., 1866 and 1759 Ma, Chen et al., 2019; Ma et al., 2020), their ages of formation do not overlap and thus they cannot be considered coeval (Figure 2a). The 1759 Ma subduction-related granites in the NL were likely linked to Proterozoic assembly of the North and West Australian Cratons (Ma et al., 2020), while the 1866 Ma arc-related magmatism in the SL was likely associated with a continental arc formed along the northern margin of India, representing a late phase in the formation of the Columbia supercontinent (Chen et al., 2019; Dong et al., 2022). The congruence between the age peaks of 2.0–1.3 Ga xenocrystic zircons in the Guomangtso Suite and contemporaneous magmatism in the Rudall Province further supports the affinity between the NL and Western Australia (Figure 2a).

The studied 2.62 Ga granites, the oldest rocks in the Lhasa terrane, occur as huge boulders embedded in nearshore deposits of the Lagar Formation. The presence of ripples and biolithic limestone intercalations of the Lagar Formation in the study area indicates a coastal, shallow sea environment. This suggests that the Neoarchean granite boulders originated from the NL or its adjacent regions. Abundant ancient xenocrystic zircons within the Guomangtso Suite imply the presence of older basement rocks (e.g., 1.9–1.3 and 3.0–2.3 Ga) beneath the NL, indicating that the 2.62 Ga granite boulders may originate from the NL itself. The 2.62 Ga riebeckite-bearing granites in the NL record zircon saturation temperatures of 860–899°C (Watson & Harrison, 1983) and are comparable to anorogenic/A-type rocks, suggesting formation in a continental rift environment.

The Pilbara Craton, situated on the edge of Western Australia, emerges as the most plausible source for the 2.62 Ga rift-related granite boulders in the NL, given that it experienced rifting and subsidence between 2.7 and 2.6 Ga (Hickman, 2012). Whole-rock Sr-Nd-Pb isotope data suggest that the NL and Western Australia share the same isotopic signatures (Figures 3d–3f), indicating that they may have been located in the same tectono-geochemical province during the pre-Neoproterozoic. Further, age peaks from 3.0 to 2.2 Ga xenocrystic zircons within the Guomangtso Suite correlate well with contemporaneous magmatism in the Pilbara Craton (Figure 2a). These findings highlight several strong and independent lines of magmatic affinity between the NL and Western Australia prior to the Neoproterozoic.

10.1029/2024GL113338

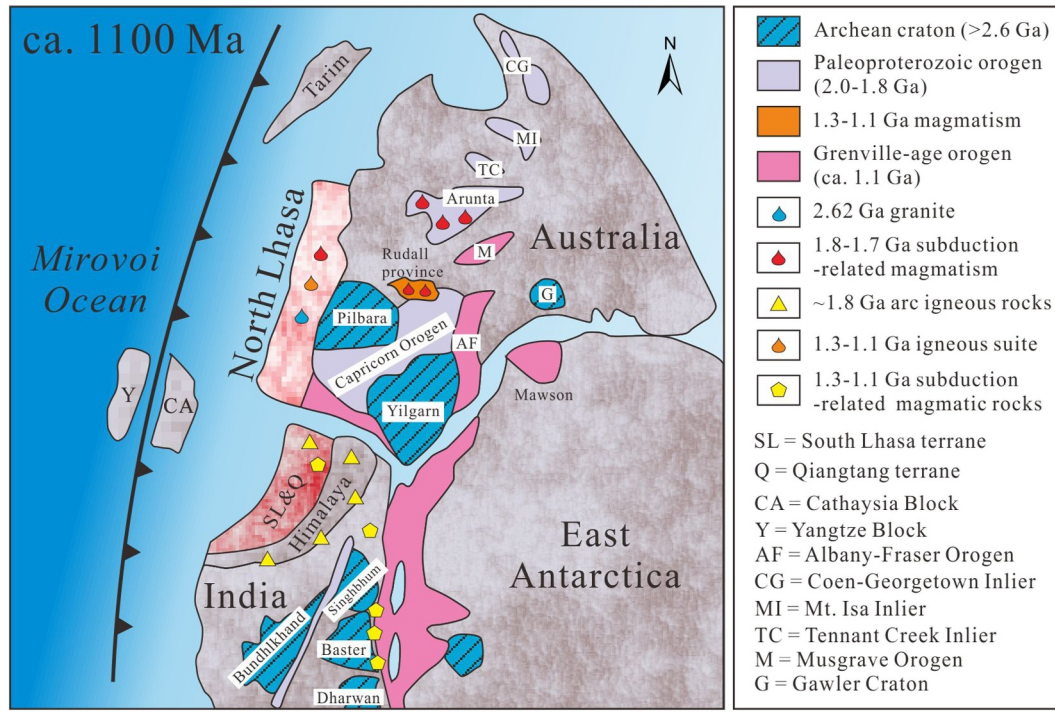

Figure 4. Reconstruction of ~1100 Ma northwestern Rodinia (modified from Ali & Aitchison, 2005; Cawood et al., 2018; Li et al., 2008; Yuan et al., 2023; Zhao et al., 2002). The locations of 2.62, 1.8–1.7, and 1.3–1.1 Ga magmatism in the North Lhasa terrane (Ma et al., 2020), ~1.8 Ga arc igneous rocks and 1.3–1.1 Ga subduction-related magmatic rocks in the South Lhasa terrane (Chen et al., 2019) are highlighted.

Previous work suggested that c. 1.17 Ga detrital zircons from Paleozoic sedimentary rocks and Neoproterozoic basement lithologies within the NL correlate with c. 1.3–1.1 Ga granitic rocks in the Albany-Fraser belt and Rudall Province, Western Australia (Yu et al., 2024; Zhu et al., 2011). However, the newly identified 1.30–1.10 Ga Guomangtso Suite in this study reveals another potential source for these detrital zircons, which may actually be the most likely source—the NL itself. Compared to having being transported from distant regions such as Australia or Africa, detrital material from the NL itself is more likely to be preserved in its own Neoproterozoic and Paleozoic strata. Despite detrital zircon analysis having non-unique interpretations, the comparison of the pre-Neoproterozoic tectono-magmatic events links the NL with Western Australia during the pre-Neoproterozoic, which resolves the contradictions caused by the multiple interpretations of detrital zircon data. As such, the original data presented here allow us to propose a comprehensive paleogeographic model for the Lhasa terrane, whereby the NL was connected with Western Australia—near the Pilbara Craton and Rudall Province—and the SL was part of India before the Neoproterozoic (Figure 4). The NL may record the assembly of the West and North Australian Cratons, as well as the 2.62 Ga rift event. In contrast, the SL experienced the growth and breakup of the Columbia supercontinent and the amalgamation of the Rodinia supercontinent (Chen et al., 2019).

4.2. Constraining the Origin of the Lhasa Terrane

Current models for the origins of India and Australia predominantly rely on detrital zircon provenance analysis, and overlook the significant differences between the Precambrian basements of the NL and SL (e.g., Gehrels et al., 2011; Guo et al., 2017; Wang et al., 2021; Zhou et al., 2019; Zhu et al., 2011). Although the origin model for Africa (Northern East African Orogen) separates the NL and SL due to the absence of pre-Neoproterozoic geological records in the NL, it primarily supported by late Neoproterozoic–Early Paleozoic geological records (Hu, Zhai, Zhao, Tang, et al., 2019; Hu et al., 2018b; Zhang et al., 2012). This model proposed here is revised based on direct comparison of pre-Neoproterozoic rocks from the SL and NL. The 2.7–2.6 Ga rift-related felsic rocks of the Fortescue Group from the Pilbara Craton (Hawkesworth & Kemp, 2021) serve as both age and geochemical analogs for the 2.62 Ga granite identified in the NL. The Rudall Province in northern Western Australia represents a Paleo-to Mesoproterozoic orogen between the North and West Australian Cratons,

recording the effects of their amalgamation (Gardiner et al., 2018). This amalgamation was recorded by 1.76 Ga tonalitic conglomerates (Ma et al., 2020) and the 1.30–1.10 Ga Guomangtso Suite found in the NL. Meanwhile, a coherent continental arc along the northern margin of India formed by the SL and Lesser Himalayan sequence at 1880–1780 Ma, with subsequent accretion and continental collision events at 1264–1250 and 1117 Ma, respectively (Figure 4; Chen et al., 2019). In contrast, pre-Neoproterozoic evidence for an Indian affinity comes from the Nyingchi Complex, which forms the Precambrian basement of the SL (Chen et al., 2019). This revised paleogeographic model and new supporting data fill in a crucial gap in the pre-Neoproterozoic evolution of the NL.

When compared to the multiple affinities proposed for the Neoproterozoic basement, information about geological origins carried by the pre-Neoproterozoic rocks of the NL coherently suggests that it is related to Western Australia. Futhermore, direct comparison between these rocks and the Precambrian basement of the SL suggests that the SL and NL have different origins, with the SL possibly originating from India. This conclusion is distinct from the existing pre-Neoproterozoic model, which posits that the Lhasa terrane was a single entity, originating from India, before the Neoproterozoic (e.g., Chen et al., 2019; Dong et al., 2022; Lin et al., 2013; Xu et al., 2013).

4.3. Significance for Neoproterozoic Reconstruction

Our recent work documented early Neoproterozoic intercontinental rift magmatic-sedimentary records within the NL (Yu et al., 2023, 2024); however, similar rifting events have also been reported in Africa and Western Australia (Hu, Zhai, Zhao, et al., 2022; Lindsay et al., 1987). Based on a series of pre-Neoproterozoic magmatic records similar to those in Western Australia, as reported here, the early Neoproterozoic rifting event in the NL should be related to Western Australia. Previous placement of the NL near Western Australia was primarily based on the comparison of early Neoproterozoic rifting events and c. 1.17 Ga detrital zircons (e.g., Yu et al., 2024; Zhu et al., 2011), which was a reasonable conclusion prior to discovery of the Guomangtso Suite. But it now seems that the NL could be an alternative source of these c. 1.17 Ga detrital zircons alongside Western Australia. The reconstructions presented here therefore build upon and clarify ambiguity releated to interpretation of previous evidence. The pre-Neoproterozoic tectonic-magmatic events related to Western Australia reported here link the early Neoproterozoic intercontinental rift in the NL with a contemporaneous rifting event in Western Australia. Therefore, the newly reported pre-Neoproterozoic rocks in this paper provide key evidence to support our earlier paleogeographic reconstruction for the NL in the early Neoproterozoic (Yu et al., 2024).

During the middle Neoproterozoic, ~800 Ma arc-related sedimentation suggests that the NL was situated on the northern margin of India (Zhou et al., 2019), while ~760-730 Ma fragments of oceanic crust connect the NL with closure of the Mozambique Ocean (Zhang et al., 2022). In the late Neoproterozoic, ~650 Ma orogenic magmatic-metamorphic records suggest a connection between the NL and Africa (Northern East African Orogen) (Zhang et al., 2012, 2022). When these three paleogeographic reconstructions are combined, they form our previously proposed three-stage evolution hypothesis for the NL (Yu et al., 2024), which involves counterclockwise rotation. The findings in this study therefore provide crucial evidence for the paleogeographic reconstruction of the earliest stage of this sequence, enhancing the credibility of the three-stage rotation model. This rotation may have facilitated the orthoversion from Rodinia to Gondwana supercontinent (Johansson, 2014; Mitchell et al., 2012; Wang et al., 2023).

5. Conclusions

This study reports newly discovered pre-Neoproterozoic rocks from the North Lhasa terrane. These rocks record mid-Neoarchean continental rifting and late Mesoproterozoic subduction-to-backarc extension-related magmatism, which can be compared to contemporaneous tectono-magmatic events in the Pilbara Craton and Rudall Province of Western Australia. However, these events differ significantly from the pre-Neoproterozoic geological records of the South Lhasa terrane, which shows a close affinity to India. Our findings suggest that the North Lhasa terrane originated from Western Australia, and that the North Lhasa and South Lhasa terranes may have distinct origins.

Data Availability Statement

The Supporting Information S1 includes detailed analytical methods, Supporting Information S1 (Figures S1–S4) and captions for the Supporting Information S1 (Tables S1–S4). All raw and processed data supporting the findings of this study are publicly available and can be accessed at https://doi.org/10.6084/m9.figshare.26054158 (Yu et al., 2025).

Acknowledgments
The authors thank the Editor and three reviewers for their comments which helped improve the manuscript. This work was supported by the China National Science and Technology Major Project (Grant 2024ZD1001104), the National Key R&D Program of China (Grant 2022YFC3080200), the National Natural Science Foundation of China (Grants 42430305, 42230303, and 42488201), the Scientific Research Project of the Education Department of Jilin Province (Grant JJKH20241254KJ), and Graduate Innovation Fund of Jilin University (Grant 2024CX102).

References

Ali, J. R., & Aitchison, J. C. (2005). Greater India. *Earth-Science Reviews*, *72*(3–4), 169–188. https://doi.org/10.1016/j.earscirev.2005.07.005

Bickle, M. J., Bettenay, L. F., Chapman, H. J., Groves, D. I., McNaughton, N. J., Campbell, I. H., & De Laeter, J. R. (1989). The age and origin of younger granitic plutons of the Shaw Batholith in the Archaean Pilbara block, western Australia. *Contributions to Mineralogy and Petrology*, *101*(3), 361–376. https://doi.org/10.1007/BF00375320

Cawood, P. A., & Korsch, R. J. (2008). Assembling Australia: Proterozoic building of a continent. *Precambrian Research*, *166*(1–4), 1–35. https://doi.org/10.1016/j.precamres.2008.08.006

Cawood, P. A., Zhao, G., Yao, J., Wang, W., Xu, Y., & Wang, Y. (2018). Reconstructing South China in Phanerozoic and Precambrian supercontinents. *Earth-Science Reviews*, *186*, 173–194. https://doi.org/10.1016/j.earscirev.2017.06.001

Chen, L. R., Xu, W. C., Zhang, H. F., Zhao, P. L., Guo, J. L., Luo, B. J., et al. (2019). Origin and early evolution of the Lhasa Terrane, South Tibet: Constraints from the Bomi Gneiss complex. *Precambrian Research*, *331*, 105360. https://doi.org/10.1016/j.precamres.2019.105360

Chen, Y. F., Zhang, Z. M., Chen, X. H., Palin, R. M., Tian, Z. L., Shao, Z. G., et al. (2022). Neoproterozoic and early Paleozoic magmatism in the eastern Lhasa terrane: Implications for Andean-type orogeny along the northern margin of Rodinia and Gondwana. *Precambrian Research*, *369*, 106520. https://doi.org/10.1016/j.precamres.2021.106520

Cutten, H. N., Thorne, A. M., & Johnson, S. P. (2011). Geology of the Edmund and collier groups. In S. P. Johnson, A. M. Thorne, & I. M. Tyler (Eds.), *Capricorn orogen seismic and magnetotelluric (MT) workshop 2011: Extended abstracts* (Vol. 25, pp. 41–48). Geological Survey of Western Australia.

Dhuime, B., Hawkesworth, C., & Cawood, P. (2011). When continents formed. *Science*, *331*(6014), 154–155. https://doi.org/10.1126/science.1201245

Dong, X., Zhang, Z., Niu, Y., Tian, Z., & Zhang, L. (2020). Reworked Precambrian metamorphic basement of the Lhasa terrane, southern Tibet: Zircon/titanite U–Pb geochronology, Hf isotope and geochemistry. *Precambrian Research*, *336*, 105496. https://doi.org/10.1016/j.precamres.2019.105496

Dong, X., Zhang, Z., & Tian, Z. (2022). Precambrian metamorphic basement of the southern Lhasa terrane, Tibet. *Precambrian Research*, *368*, 106478. https://doi.org/10.1016/j.jog.2011.05.002

Gardiner, N. J., Hickman, A. H., Kirkland, C. L., Lu, Y., Johnson, T., & Zhao, J. X. (2017). Processes of crust formation in the early Earth imaged through Hf isotopes from the East Pilbara Terrane. *Precambrian Research*, *297*, 56–76. https://doi.org/10.1016/j.precamres.2017.05.004

Gardiner, N. J., Maidment, D. W., Kirkland, C. L., Bodorkos, S., Smithies, R. H., & Jeon, H. (2018). Isotopic insight into the Proterozoic crustal evolution of the Rudall province, western Australia. *Precambrian Research*, *313*, 31–50. https://doi.org/10.1016/j.precamres.2018.05.003

Gehrels, G. E., Kapp, P., DeCelles, P., Pullen, A., Blakey, R., Weislogel, A., et al. (2011). Detrital zircon geochronology of pre-Tertiary strata in the Tibetan Himalayan orogen. *Tectonics*, *30*(5). https://doi.org/10.1029/2011TC002868

Guo, L., Zhang, H. F., Harris, N., Xu, W. C., & Pan, F. B. (2017). Detrital zircon U–Pb geochronology, trace-element and Hf isotope geochemistry of the metasedimentary rocks in the eastern Himalayan syntaxis: Tectonic and paleogeographic implications. *Gondwana Research*, *41*, 207–221. https://doi.org/10.1016/j.gr.2015.07.013

Hartnady, M. I., Kirkland, C. L., Smithies, R. H., Johnson, S. P., & Johnson, T. E. (2022). Pb isotope insight into the formation of the Earth's first stable continents. *Earth and Planetary Science Letters*, *578*, 117319. https://doi.org/10.1016/j.epsl.2021.117319

Hawkesworth, C., & Kemp, T. (2021). A Pilbara perspective on the generation of Archaean continental crust. *Chemical Geology*, *578*, 120326. https://doi.org/10.1016/j.chemgeo.2021.120326

Hickman, A. H. (2012). Review of the Pilbara craton and Fortescue basin, western Australia: Crustal evolution providing environments for early life. *Island Arc*, *21*(1), 1–31. https://doi.org/10.1111/j.1440-1738.2011.00783.x

Honarmand, M., Xiao, W., Nabatian, G., Blades, M. L., dos Santos, M. C., Collins, A. S., & Ao, S. (2018). Zircon U-Pb-Hf isotopes, bulk-rock geochemistry and Sr-Nd-Pb isotopes from late Neoproterozoic basement in the Mahneshan area, NW Iran: Implications for Ediacaran active continental margin along the northern Gondwana and constraints on the late Oligocene crustal anatexis. *Gondwana Research*, *57*, 48–76. https://doi.org/10.1016/j.gr.2017.12.009

Hu, P. Y., Zhai, Q. G., Cawood, P. A., Weinberg, R. F., Zhao, G. C., Tang, Y., & Liu, Y. M. (2023). Paleogeographic reconstruction of Precambrian terranes reworked by Phanerozoic orogens: An example based on detrital zircon REE from Lhasa terrane in southern Tibet. *Geophysical Research Letters*, *50*(5), e2023GL102979. https://doi.org/10.1029/2023GL102979

Hu, P. Y., Zhai, Q. G., Cawood, P. A., Zhao, G. C., Wang, J., Tang, Y., et al. (2021). Cambrian magmatic flare-up, central Tibet: Magma mixing in proto-Tethyan arc along north Gondwanan margin. *Geological Society of America Bulletin*, *133*(9–10), 2171–2188. https://doi.org/10.1130/B35859.1

Hu, P. Y., Zhai, Q. G., Cawood, P. A., Zhao, G. C., Wang, J., Tang, Y., et al. (2022). Middle Neoproterozoic (ca. 700 Ma) tectonothermal events in the Lhasa terrane, Tibet: Implications for paleogeography. *Gondwana Research*, *104*, 252–264. https://doi.org/10.1016/j.gr.2021.01.014

Hu, P. Y., Zhai, Q. G., Wang, J., Tang, Y., Wang, H. T., & Hou, K. J. (2018a). Precambrian origin of the North Lhasa terrane, Tibetan Plateau: Constraint from early Cryogenian back-arc magmatism. *Precambrian Research*, *313*, 51–67. https://doi.org/10.1016/j.precamres.2018.05.014

Hu, P. Y., Zhai, Q. G., Wang, J., Tang, Y., Wang, H. T., & Hou, K. J. (2018d). Ediacaran magmatism in the North Lhasa terrane, Tibet and its tectonic implications. *Precambrian Research*, *307*, 137–154. https://doi.org/10.1016/j.precamres.2018.01.012

Hu, P. Y., Zhai, Q. G., Wang, J., Tang, Y., Wang, H. T., Zhu, Z. C., & Wu, H. (2018b). Middle Neoproterozoic (ca. 760 Ma) arc and back-arc system in the North Lhasa terrane, Tibet, inferred from coeval N-MORB- and arc-type gabbros. *Precambrian Research*, *316*, 275–290. https://doi.org/10.1016/j.precamres.2018.08.022

Hu, P. Y., Zhai, Q. G., Zhao, G. C., Tang, Y., Wang, H. T., Zhu, Z. C., et al. (2019). Middle Neoproterozoic magmatic event in the western Nam Tso area, Tibetan Plateau: Constraint on the origin of the North Lhasa terrane. *Acta Petrologica Sinica*, *35*(10), 3115–3129. https://doi.org/10.18654/1000-0569/2019.10.10

Hu, P. Y., Zhai, Q. G., Zhao, G. C., Tang, Y., Yang, N., & Li, J. Y. (2022). Constraints of Precambrian basement in Ren Co area, Tibet on the origin of the North Lhasa terrane. *Acta Petrologica et Mineralogica*, *41*(2), 281–302. https://doi.org/10.3969/j.issn.1000-6524.2022.02.006

Hu, P. Y., Zhai, Q. G., Zhao, G. C., Wang, J., Tang, Y., Wang, H. T., et al. (2018c). Early Neoproterozoic (ca. 900 Ma) rift sedimentation and mafic magmatism in the North Lhasa Terrane, Tibet: Paleogeographic and tectonic implications. *Lithos*, *320*, 403–415. https://doi.org/10.1016/j.lithos.2018.09.036

Hu, P. Y., Zhai, Q. G., Zhao, G. C., Wang, J., Tang, Y., Wang, H. T., et al. (2019). Late Cryogenian magmatic activity in the North Lhasa terrane, Tibet: Implication of slab break-off process. *Gondwana Research*, *71*, 129–149. https://doi.org/10.1016/j.gr.2019.02.005

Johansson, Å. (2014). From Rodinia to Gondwana with the "SAMBA" model—A distant view from Baltica towards Amazonia and beyond. *Precambrian Research*, *244*, 226–235. https://doi.org/10.1016/j.precamres.2013.10.012

Kemp, A. I., Vervoort, J. D., Petersson, A., Smithies, R. H., & Lu, Y. (2023). A linked evolution for granite-greenstone terranes of the Pilbara Craton from Nd and Hf isotopes, with implications for Archean continental growth. *Earth and Planetary Science Letters*, *601*, 117895. https://doi.org/10.1016/j.epsl.2022.117895

Kieffer, B., Arndt, N., Lapierre, H., Bastien, F., Bosch, D., Pecher, A., et al. (2004). Flood and shield basalts from Ethiopia: Magmas from the African superswell. *Journal of Petrology*, *45*(4), 793–834. https://doi.org/10.1093/petrology/egg112

Li, Z. X., Bogdanova, S., Collins, A., Davidson, A., De Waele, B., Ernst, R., et al. (2008). Assembly, configuration, and break-up history of Rodinia: A synthesis. *Precambrian Research*, *160*(1–2), 179–210. https://doi.org/10.1016/j.precamres.2007.04.021

Lin, Y. H., Zhang, Z. M., Dong, X., Shen, K., & Lu, X. (2013). Precambrian evolution of the Lhasa terrane, Tibet: Constraint from the zircon U–Pb geochronology of the gneisses. *Precambrian Research*, *237*, 64–77. https://doi.org/10.1016/j.precamres.2013.09.006

Lindsay, J. F., Korsch, R. J., & Wilford, J. R. (1987). Timing the breakup of a Proterozoic supercontinent: Evidence from Australian intracratonic basins. *Geology*, *15*(11), 1061–1064. https://doi.org/10.1130/0091-7613(1987)15<1061:TTBOAP>2.0.CO;2

Ma, D. S., Xiong, X. G., Zeng, Y. R., Fu, H. B., & Guo, H. (2015). The discovery of volcanics intercalation in Upper Carboniferous-Lower Permian Laka formation, Tarezeng area, Tibet. *Geological Bulletin of China*, *34*, 1636–1644. [in Chinese with English abstract].

Ma, J., An, X., Huang, F., Li, Y., Zhang, Y., & Zhu, T. (2020). Provenance of glacial marine conglomerates in the Permian Lagar Formation of southern Tibet: Evidence for affinity of the Lhasa terrane with Australia. *Journal of Asian Earth Sciences*, *187*, 104064. https://doi.org/10.1016/j.jseaes.2019.104064

Martin, D. M., & Thorne, A. (2004). Tectonic setting and basin evolution of the Bangemall Supergroup in the northwestern Capricorn orogen. *Precambrian Research*, *128*(3–4), 385–409. https://doi.org/10.1016/j.precamres.2003.09.009

Mitchell, R. N., Kilian, T. M., & Evans, D. A. (2012). Supercontinent cycles and the calculation of absolute palaeolongitude in deep time. *Nature*, *482*(7384), 208–211. https://doi.org/10.1038/nature10800

Payne, J. L., Morrissey, L. J., Tucker, N. M., Roche, L. K., Szpunar, M. A., & Neroni, R. (2021). Granites and gabbros at the dawn of a coherent Australian continent. *Precambrian Research*, *359*, 106189. https://doi.org/10.1016/j.precamres.2021.106189

Stoeser, D. B., & Frost, C. D. (2006). Nd, Pb, Sr, and O isotopic characterization of Saudi Arabian shield terranes. *Chemical Geology*, *226*(3–4), 163–188. https://doi.org/10.1016/j.chemgeo.2005.09.019

Veevers, J. J., Saeed, A., Belousova, E. A., & Griffin, W. L. (2005). U-Pb ages and source composition by Hf-isotope and trace-element analysis of detrital zircons in Permian sandstone and modern sand from southwestern Australia and a review of the paleogeographical and denudational history of the Yilgarn Craton. *Earth-Science Reviews*, *68*(3–4), 245–279. https://doi.org/10.1016/j.earscirev.2004.05.005

Wang, C., Jing, X. Q., & Meert, J. G. (2023). Neoproterozoic reorganization of the Circum-Mozambique orogens and growth of megacontinent Gondwana. *Communications Earth & Environment*, *4*(1), 216. https://doi.org/10.1038/s43247-023-00883-6

Wang, M., Zeng, X. W., Xie, C. M., Danzeng, A., Li, C., Fan, J. J., & Li, H. (2020). Dating of detrital zircon grains and fossils from Late Palaeozoic sediments of the Baruo area, Tibet: Constraints on the late Palaeozoic evolution of the Lhasa terrane. *International Geology Review*, *62*(4), 465–478. https://doi.org/10.1080/00206814.2019.1619199

Wang, Q., Zhu, D. C., Cawood, P. A., Chung, S. L., & Zhao, Z. D. (2021). Resolving the paleogeographic puzzle of the Lhasa terrane in southern Tibet. *Geophysical Research Letters*, *48*(15), e2021GL094236. https://doi.org/10.1029/2021GL094236

Watson, E. B., & Harrison, T. M. (1983). Zircon saturation revisited: Temperature and composition effects in a variety of crustal magma types. *Earth and Planetary Science Letters*, *64*(2), 295–304. https://doi.org/10.1016/0012-821X(83)90211-X

Whalen, J. B., Currie, K. L., & Chappell, B. W. (1987). A-Type granites: Geochemical characteristics, discrimination and petrogenesis. *Contributions to Mineralogy and Petrology*, *95*(4), 407–419. https://doi.org/10.1007/BF00402202

Xu, W. C., Zhang, H. F., Harris, N., Guo, L., Pan, F. B., & Wang, S. (2013). Geochronology and geochemistry of Mesoproterozoic granitoids in the Lhasa terrane, south Tibet: Implications for the early evolution of Lhasa terrane. *Precambrian Research*, *236*, 46–58. https://doi.org/10.1016/j.precamres.2013.07.016

Yu, C. S., Wang, M., Shen, D., Zeng, X. W., & Li, H. (2023). Response of the North Lhasa terrane to the initial break-up of Rodinia: Evidence from the newly identified early Neoproterozoic gabbros in the Asa area, southern Tibet. *Precambrian Research*, *386*, 106971. https://doi.org/10.1016/j.precamres.2023.106971

Yu, C. S., Wang, M., Shen, D., Lin, M. X., Zhang, S. S., Yang, R., & Quewang, D. (2024). North Lhasa terrane in the Precambrian originated from western Australia. *Precambrian Research*, *405*, 107371. https://doi.org/10.1016/j.precamres.2024.107371

Yu, C. S., Wang, M., Zhou, J. B., Richard, M. P., Liu, J., Wan, B., et al. (2025). Australian Heritage for the North Lhasa terrane [Dataset]. *figshare*. https://doi.org/10.6084/m9.figshare.26054158

Yuan, J., Deng, C., Yang, Z., Krijgsman, W., Qin, H., Yi, L., et al. (2023). New paleomagnetic data from the central Tethyan Himalaya refine the size of Greater India during the Campanian. *Earth and Planetary Science Letters*, *622*, 118422. https://doi.org/10.1016/j.epsl.2023.118422

Zhang, X. Z., Wang, Q., Dan, W., & Wyman, D. (2022). Locating Lhasa terrane in the Rodinia and Gondwana supercontinents. A key piece of the reconstruction puzzle. *Geological Society of America Bulletin*, *135*(1–2), 67–80. https://doi.org/10.1130/B36152.1

Zhang, Y. C., Shi, G. R., & Shen, S. Z. (2013). A review of Permian stratigraphy, palaeobiogeography and palaeogeography of the Qinghai–Tibet Plateau. *Gondwana Research*, *24*(1), 55–76. https://doi.org/10.1016/j.gr.2012.06.010

Zhang, Z. M., Dong, X., Liu, F., Lin, Y. H., Yan, R., He, Z. Y., & Santosh, M. (2012). The making of Gondwana: Discovery of 650 Ma HP granulites from the North Lhasa, Tibet. *Precambrian Research*, *212*, 107–116. https://doi.org/10.1016/j.precamres.2012.04.018

Zhao, G. C., Cawood, P. A., Wilde, S. A., & Sun, M. (2002). Review of global 2.1–1.8 Ga orogens: Implications for a pre-Rodinia supercontinent. *Earth-Science Reviews*, *59*(1–4), 125–162. https://doi.org/10.1016/S0012-8252(02)00073-9

Zhou, X., Zheng, J. P., Li, Y. B., Griffin, W. L., Xiong, Q., Moghadam, H. S., & O'Reilly, S. Y. (2019). Neoproterozoic sedimentary rocks track the location of the Lhasa Block during the Rodinia breakup. *Precambrian Research*, *320*, 63–77. https://doi.org/10.1016/j.precamres.2018.10.005

Zhu, D. C., Zhao, Z. D., Niu, Y. L., Dilek, Y., & Mo, X. X. (2011). Lhasa terrane in southern Tibet came from Australia. *Geology*, *39*(8), 727–730. https://doi.org/10.1130/G31895.1

References From the Supporting Information

Andersen, T. (2002). Correction of common lead in U-Pb analyses that do not report 204Pb. *Chemical Geology*, *192*(1–2), 59–79. https://doi.org/10.1016/S0009-2541(02)00195-X

Bouvier, A., Vervoort, J. D., & Patchett, P. J. (2008). The Lu-Hf and Sm-Nd isotopic composition of CHUR: Constraints from unequilibrated chondrites and implications for the bulk composition of terrestrial planets. *Earth and Planetary Science Letters*, *273*(1–2), 48–57. https://doi.org/10.1016/j.epsl.2008.06.010

Frost, B. R., Barnes, C. G., Collins, W. J., Arculus, R. J., Ellis, D. J., & Frost, C. D. (2001). A geochemical classification for granitic rocks. *Journal of Petrology*, *42*(11), 2033–2048. https://doi.org/10.1093/petrology/42.11.2033

Griffin, W. L., Wang, X., Jackson, S. E., Pearson, N. J., O'Reilly, S. Y., Xu, X., & Zhou, X. (2002). Zircon geochemistry and magma mixing, SE China: In-situ analysis of Hf isotopes, Tonglu and Pingtan igneous complexes. *Lithos*, *61*(3–4), 237–269. https://doi.org/10.1016/S0024-4937(02)00082-8

Hao, Y. J., Ren, Y. S., Zhao, H. L., Lai, K., Zhao, X., & Ma, Y. P. (2018). Metallogenic mechanism and tectonic setting of Tungsten Mineralization in the Yangbishan deposit in Northeastern China. *Acta Geologica Sinica-English Edition*, *92*(1), 241–267. https://doi.org/10.1111/1755-6724.13504

Hou, K. J., Li, Y. H., Zou, T. R., Qu, X. M., Shi, Y. R., & Xie, G. Q. (2007). Laser ablation–MC–ICP–MS technique for Hf isotope microanalysis of zircon and its geological applications. *Acta Petrologica Sinica*, *23*, 2595–2604. https://doi.org/10.1631/jzus.2007.B0900

Li, W. Q. (2019). Testing accuracy of 10 major elements in diabase by borate melting sample preparation method. *World Geology*, *38*, 843–851. [in Chinese with English abstract].

Li, X., Tang, G., Gong, B., Yang, Y., Hou, K., Hu, Z., et al. (2013). Qinghu zircon: A working reference for microbeam analysis of U-Pb age and Hf and O isotopes. *Chinese Science Bulletin*, *58*(36), 4647–4654. https://doi.org/10.1007/s11434-013-5932-x

Liu, Y. S., Hu, Z. C., Zong, K. Q., Gao, C. G., Gao, S., Xu, J., & Chen, H. H. (2010). Reappraisement and refinement of zircon U-Pb isotope and trace element analyses by LA-ICP-MS. *Chinese Science Bulletin*, *55*(15), 1535–1546. https://doi.org/10.1007/s11434-010-3052-4

Ludwig, K. R. (2012). *Isoplot/Ex version 4.15, a geochronological toolkit for Microsoft Excel* (Vol. 4). Berkeley Geochronology Center Special Publication.

Pearce, J. A., & Norry, M. J. (1979). Petrogenetic implications of Ti, Zr, Y, and Nb Variations in Volcanic rocks. *Contributions to Mineralogy and Petrology*, *69*(1), 33–47. https://doi.org/10.1007/BF00375192

Pearce, J. A., Harris, N. B. W., & Tindle, A. G. (1984). Trace element discrimination diagrams for the tectonic interpretation of granitic rocks. *Journal of Petrology*, *25*(4), 956–983. https://doi.org/10.1093/petrology/25.4.956

Rickwood, P. C. (1989). Boundary lines within petrologic diagrams which use oxides of major and minor elements. *Lithos*, *22*(4), 247–263. https://doi.org/10.1016/0024-4937(89)90028-5

Shervais, J. W. (1982). Ti-V plots and the petrogenesis of modern and ophiolitic lavas. *Earth and Planetary Science Letters*, *59*(1), 101–118. https://doi.org/10.1016/0012-821X(82)90120-0

Sláma, J., Košler, J., Condon, D. J., Crowley, J. L., Gerdes, A., Hanchar, J. M., et al. (2008). Plešovice zircon - A new natural reference material for U-Pb and Hf isotopic microanalysis. *Chemical Geology*, *249*(1–2), 1–35. https://doi.org/10.1016/j.chemgeo.2007.11.005

Soderlund, U., Patchett, P. J., Vervoort, J. D., & Isachsen, C. E. (2004). The 176Lu decay constant determined by Lu–Hf and U-Pb isotope systematics of Precambrian mafic intrusions. *Earth and Planetary Science Letters*, *219*(3–4), 311–324. https://doi.org/10.1016/S0012-821X(04)00012-3

Spencer, C. J., Kirkland, C. L., & Taylor, R. J. M. (2016). Strategies towards statistically robust interpretations of in situ U-Pb zircon geochronology. *Geoscience Frontiers*, *7*(4), 581–589. https://doi.org/10.1016/j.gsf.2015.11.006

White, W. M., Albarède, F., & Télouk, P. (2000). High-precision analysis of Pb isotope ratios by multi-collector ICP-MS. *Chemical Geology*, *167*(3–4), 257–270. https://doi.org/10.1016/S0009-2541(99)00182-5

Wiedenbeck, M., Alle, P., Corfu, F., Griffin, W. L., Meier, M., Oberli, F., et al. (1995). Three natural zircon standards for U-Th-Pb, Lu-Hf, trace-element and REE analyses. *Geostandards Newsletter*, *19*, 1–23. https://doi.org/10.1111/j.1751-908X.1995.tb00147.x

Yang, Y. H., Zhang, H. F., Chu, Z. Y., Xie, L. W., & Wu, F. Y. (2010). Combined chemical separation of Lu, Hf, Rb, Sr, Sm and Nd from a single rock digest and precise and accurate isotope determinations of Lu-Hf, Rb-Sr and Sm-Nd isotope systems using Multi-Collecter ICP-MS and TIMS. *International Journal of Mass Spectrometry*, *290*(2–3), 120–126. https://doi.org/10.1016/j.ijms.2009.12.011